Jennifer M. Wilson*, Ionut Mihalcea, Mario Veicht, Đorđe Cvjetinović and Dorothea Schumann

Recovery of no-carrier-added ^{41}Ca, ^{44}Ti, and ^{26}Al from high-energy proton-irradiated vanadium targets

https://doi.org/10.1515/ract-2022-0072
Received July 11, 2022; accepted December 21, 2022;
published online January 19, 2023

Abstract: Many useful and needed radionuclides for medicinal, astrophysical, and environmental research are produced naturally in inefficient quantities or not-at-all. In the method described here, rare cosmogenic isotopes were produced via spallation reactions in metallic vanadium and separated without adding any carriers. In the SINQ facility at the Paul Scherrer Institut, the vanadium targets were irradiated for two years with high-energy protons (≤590 MeV). After a cooling period of eight years, only relatively long-lived radionuclides such as ^{32}Si, ^{44}Ti, ^{41}Ca, and ^{26}Al remain present. After target dissolution, ^{32}Si was first separated for a prospective half-life redetermination. The remaining ^{32}Si-free solution was used for extracting ^{44}Ti, ^{41}Ca, and ^{26}Al, three key isotopes which are scientifically interesting for nuclear astrophysics research as well as medical applications. Each separation scheme employed ion-exchange and extraction chromatography; developed and optimized using inactive model solutions analyzed with Inductively Coupled Plasma–Optical Emission Spectrometry (ICP–OES). The irradiated samples were tracked with γ-ray spectroscopy for γ-ray emitting impurities. As a result, radiochemically pure sample solutions of ^{44}Ti, ^{41}Ca, and ^{26}Al were obtained as "ready for use" in different application fields.

Keywords: extraction chromatography; ion chromatography; isotope production; no-carrier-added radionuclides; radiochemical separation.

1 Introduction

In a previous paper [1], we reported on the separation of ^{32}Si from vanadium disks, which had been irradiated with high-energetic protons in the Swiss Spallation Neutron Source (SINQ) target at PSI for two years. The work was aimed at providing enough sample material for a reliable redetermination of the ^{32}Si half-life. The remaining solution contained, among others, three exotic carrier-free nuclides: ^{44}Ti, ^{41}Ca, and ^{26}Al, which are of particular interest in several fields of nuclear science:

(i) Typically, ^{44}Ti is formed via nucleosynthesis in supernovae [2]. It decays via electron capture (EC) and has an associated dual γ-ray emission used for young supernovae identification [2, 3]. Its half-life, $t_{1/2}$ = 59.1 (3) yr [4], prevents the nuclide from being directly seen in meteorites since its travel time to Earth is much longer than the life of ^{44}Ti. Instead, the large excesses of its stable granddaughter, ^{44}Ca, indirectly quantifies ^{44}Ti [5, 6]. Medically, ^{44}Ti is sought after as the parent for the ^{44}Ti/^{44}Sc generator [7]. ^{44}Sc decays via EC and β+ emission ($t_{1/2}$ = 3.97 (4) hr [4]) and is an ideal candidate for Positron Emission Tomography (PET). Most PET isotopes require on-site production via cyclotron, subsequent separation, and preparation for medical applications. A nuclide generator widens the number of facilities able to use PET without a cyclotron [7]. Fortunately, ^{44}Ti only decays to ^{44}Sc, rather than the longer-lived ^{44m}Sc ($t_{1/2}$ = 58.61 (10) hr [4]). The benefits of ^{44}Sc as a PET nuclide are: a short half-life, a biologically friendly stable daughter ^{44}Ca, and, necessary for a generator, a mother with a half-life longer than the daughter nuclide.

(ii) ^{41}Ca is mainly formed within supernovae [6] and is an ideal candidate for nuclear dating because its half-life

present address: Jennifer M. Wilson, Department of Chemistry and Applied Biosciences, Laboratory of Inorganic Chemistry, ETH Zürich, Zürich, Switzerland

***Corresponding author: Jennifer M. Wilson,** Laboratory of Radiochemistry, Paul Scherrer Institut (PSI), Forschungsstrasse 111, 5232 Villigen, Switzerland; and Department of Chemistry, Biochemistry, and Pharmaceutical Sciences, University of Bern, Hochschulstrasse 6, 3012 Bern, Switzerland, E-mail: jennifer.wilson@psi.ch
Ionut Mihalcea and Dorothea Schumann, Laboratory of Radiochemistry, Paul Scherrer Institut (PSI), Forschungsstrasse 111, 5232 Villigen, Switzerland, E-mail: dorothea.schumann@psi.ch (D. Schumann)
Mario Veicht, Laboratory of Radiochemistry, Paul Scherrer Institut (PSI), Forschungsstrasse 111, 5232 Villigen, Switzerland; and École Polytechnique Fédérale de Lausanne (EPFL), Route Cantonale, 1015 Lausanne, Switzerland, E-mail: mario-aaron.veicht@psi.ch
Đorđe Cvjetinović, Laboratory of Radiochemistry, Paul Scherrer Institut (PSI), Forschungsstrasse 111, 5232 Villigen, Switzerland; and Faculty of Physical Chemistry, University of Belgrade, Studentski trg 12-16, 11158 Belgrade, Serbia, E-mail: djorde.cvjetinovic@psi.ch

($9.94\ (15) \times 10^4$ yr [8]) bridges the age gap between two commonly used dating radionuclides, ^{14}C and ^{36}Cl ($t_{1/2} = 5.700\ (30) \times 10^3$ yr and $3.013\ (15) \times 10^5$ yr respectively) [9]. In addition, ^{41}Ca can be used as a long-term medical tracer for sorption within bones [10]. For accurate analysis, large quantities of ^{41}Ca for standards are necessary to date meteorites [6], bones [11], and limestone [12].

(iii) ^{26}Al ($t_{1/2} = 7.17\ (24) \times 10^5$ yr) decays via EC and β+ with an associated γ-ray emission [13]. Like the preceding nuclides, it plays a role in nuclear astrophysical research where the information gained from ^{26}Al γ-ray analysis ranges from nucleosynthesis [14] to the supernova explosion of massive stars [6]. It is also cosmogenically formed through neutron-induced spallation of argon in the atmosphere [15] or through muon interactions in quartz [16]. Its constant surface production allows dating with ^{26}Al/^{10}Be isotope ratios within ice [17] and caves [18].

In order to study the nuclear astrophysics processes described above as well as for establishing these nuclides as environmental dating tools, sufficient sample amounts in the requested quality fitting to the specific envisaged experiment – for instance cross section measurements or determination of nuclear decay properties like half-lives, emission probabilities or branching ratios – are urgently needed. Complementary production routes exist for all three isotopes. ^{41}Ca can easily be produced via neutron activation of ^{40}Ca in a nuclear reactor, but the reaction product contains large amounts of stable Ca, preventing from its use in many applications. Non-carrier added ^{44}Ti can be obtained by proton irradiation of natural scandium as explored by [7]. The challenge with this approach is that the daughter nuclide of the generator is the same element as the target material, so that extremely high separation of the titanium from the scandium is required. ^{41}Ca and ^{26}Al can also be produced in (p,n) reactions, but the natural abundances of the needed target materials, ^{41}K and ^{26}Mg, are only 6.7% and 11%, respectively. To some extent, this reduces the advantage of the higher cross sections. Moreover, highly enriched material has to be used to suppress the production of unwanted by-products. The advantage of isotope production using the SINQ target at PSI is the vast range of interesting isotopes and the beam time for free. This outweighs the effort to develop and perform the more complicated chemical separations.

The excitation functions for all three isotopes from proton-irradiated vanadium have been determined earlier [19, 20]. For ^{44}Ti, no chemical separation was needed because of the good measurability of the radiation [19], however ^{41}Ca and ^{26}Al both required chemical separation prior to detection [20]. A key difference between the separation procedures presented here and by the other authors [20] is the irradiated vanadium targets here were approximately three times larger and irradiated longer. As a result, separations occurred from a larger vanadium matrix with more undesired radionuclides within the irradiated samples. Presented here is the separation of ^{41}Ca, ^{44}Ti, and ^{26}Al from a vanadium matrix solution via chromatographic separation methods after the previous removal of ^{32}Si, reported earlier [1].

2 Experimental studies

2.1 Materials and instruments

All separations and purifications utilized ion-exchange and extraction column chromatography. Titanium and calcium separations exclusively used extraction resins, whereas aluminum separations required a series of ion-exchange and extraction resins. For the ion-exchange experiments, Dowex® resins were used for both cation- (Dowex® 50WX8 resin, 200–400 mesh, Sigma-Aldrich, Germany) and anion-exchanges (Dowex® 1X8 resin, 200–400 mesh, Sigma-Aldrich, Germany). The extraction resins (TrisKem SAS, Bruz, France) were normal DGA (50–100 µm), LN1 (20–50 µm), and LN3 (20–50 µm). Each experiment was optimized first with non-irradiated metallic vanadium disks identical to the irradiated targets (Ø = 9 mm, 1 mm thick, ≈417 ± 4 mg, chemical purity: 99.8% V, Goodfellow Cambridge Limited, U.K.). Single element standards (1000 mg/L in 2% HNO_3, Sigma-Aldrich, Germany) were used to develop the separation methods. Preconditioning and eluents were diluted HNO_3 (69 wt%, Honeywell, U.S.A.) or HF (40 wt%, Merck, Germany) prepared with ultra-pure water (upt-H_2O, 18.2 MΩ × cm, Veolia S.A.).

Each setup utilized an in-house made pressurized column apparatus comprised of: the chosen resin, polymethyl methacrylate columns (inner-Ø = 10 mm, and 300 or 100 mm length), squeeze tubes (Ismaprene PharMed®, Cole-Parmer Instrument Company, LLC., U.S.A.), PE frits (Ø = 10 mm, 30 µm pore-size, Kinesis Group from Cole-Parmer Instrument Company, LLC., U.S.A.), and a peristaltic pump (REGLO Digital MS-2/8, Cole-Parmer Instrument Company, LLC., U.S.A.).

For the analysis during method development, ICP–OES (Agilent 5110, Agilent Technologies, U.S.A) was employed using inactive solutions. The associated breakthrough curves can be viewed in the Supplementary Material (SM). The irradiated samples were tracked via γ-ray spectrometry using a high-purity germanium (HPGe) detector (Mirion Technologies, California, U.S.A.) as well as via liquid scintillation counting (LSC) using a Packard Tri-Carb® 2250CA.

2.2 Irradiation and first separation

At the SINQ facility of PSI, 150 vanadium targets were irradiated for two years under a high-energy proton beam (≤590 MeV) [21]. The Gaussian shaped beam irradiated the stacked targets perpendicular to the stack lengthwise, thus each target was subjected to a different power intensity resulting in a different composition of radionuclides per target [22]. After irradiation, the targets were placed in intermediate storage for eight years without previous measurement. The initial target dissolution and first chromatographic separation of ^{32}Si via cation-exchange

chromatography are described elsewhere [1], thus not a subject in this study. After the ^{32}Si removal, ^{41}Ca, ^{44}Ti, ^{26}Al, and the vanadium bulk remained in 50 mL 3 M HNO_3, the starting solution for the proceeding separations.

2.3 General separation procedure

Unless otherwise stated, all chromatographic separations were carried out according to the following outline. Before assembly, each resin was saturated in upt-H_2O for at least 24 h, then added into the column, held between two PE frits. Solutions were introduced through a feeder connected to a peristaltic pump with squeeze tubing maintained at 1.50 mL/min. Prior to the experiments, the resins were pre-conditioned with the solvent of the loading solution; stated for each separation specifically. The experiments then followed these general steps: (i) the loading solution containing all matrix elements (Load), (ii) a wash of the same solvent (Wash), (iii) a chosen eluent solution to wash-off desired elements (Elute), and eventually (iv) one or more consecutive solutions preparing the resin for reuse (post-conditioning). Unless otherwise stated, the Load and Wash were collected together in preparation for the subsequent element separation. However, the Elute was further utilized for purification procedures.

2.4 Calcium separation

For the calcium separation from vanadium, a 30 mm high resin bed of DGA resin was preconditioned with 10 mL 3 M HNO_3 solution. The initial vanadium solution after ^{32}Si separation [1] was used as the Load without further manipulation. The Load, 50 mL 3 M HNO_3, and Wash, 20 mL 3 M HNO_3, were collected for further separations. Calcium was eluted with 20 mL upt-H_2O, followed by 10 mL 3 M HNO_3 post-conditioning.

The calcium fractions then underwent two purification steps, where the second step additionally served to concentrate the calcium fraction (see Figure 1). The collected Elute from the bulk vanadium separation was acidified with 0.66 mL conc. HNO_3 to reach a 20.66 mL 0.5 M HNO_3 Load. The LN3 resin (bed height: 30 mm) was preconditioned with 10 mL 0.5 M HNO_3, followed by the Load and 5 mL 0.5 M HNO_3 Wash. The Load and Wash were collected together for the next purification step. In preparation for resin reuse, 15 mL upt-H_2O then 10 mL 0.5 M HNO_3 were added as post-conditioning.

Finally, the solution was purified and concentrated using DGA resin (bed height: 30 mm). Here, the Load was the collected Load and Wash from the previous purification on LN3 resin, 25.66 mL 0.5 M HNO_3, which was then acidified with 0.876 mL conc. HNO_3 to reach 1 M HNO_3. The calcium solutions from 10 vanadium targets were used as the Load (approx. 265 mL 1 M HNO_3). The resin was preconditioned with 15 mL 1 M HNO_3 before adding the ≈265 mL Load, 20 mL 1 M HNO_3 Wash, 20 mL utp-H_2O Elute (final ^{41}Ca solution), then 15 mL 1 M HNO_3 post-conditioning.

2.5 Titanium separation

The 70 mL 3 M HNO_3 Load and Wash obtained from the calcium separation from vanadium was used directly as the Load solution here. First, the LN1 extraction resin (bed height: 20 mm) was preconditioned with 15 mL 3 M HNO_3. Sequentially, the 70 mL Load, 20 mL 3 M HNO_3 Wash, and 20 mL 1 M HF Elute were fed through the column (see Figure 1). The Load and Wash were collected for the separation of aluminum. Following the elution, 10 mL upt-H_2O and 15 mL 3 M HNO_3 were used to prepare the resin for a subsequent vanadium solution.

2.6 Aluminum separation

Here, the aluminum separation from the vanadium matrix was optimized utilizing a two-step cation exchange. For Step #1, the 90 mL 3 M HNO_3 Load and Wash from the titanium separation from vanadium was diluted to 1.5 M HNO_3 with 90 mL upt-H_2O as the first Load. A 210 mm resin bed height column was preconditioned with 20 mL 1.5 M HNO_3 followed by the 180 mL Load and 30 mL 1.5 M HNO_3 Wash. The Elute, 40 mL 5 M HNO_3, was collected in two separate 20 mL fractions; the Load and Wash were discarded (see Figure 2, Step #1).

In preparation for Step #2, each collected Elute fraction from Step #1 was diluted to 1.25 M with 60 mL upt-H_2O. These solutions were then used as the Load for Step #2 in the same order as collection in Step #1 (see Figure 2). For Step #2, a 130 mm resin bed height column was preconditioned with 20 mL 1.25 M HNO_3 followed by: both Loads, 2 × 80 mL

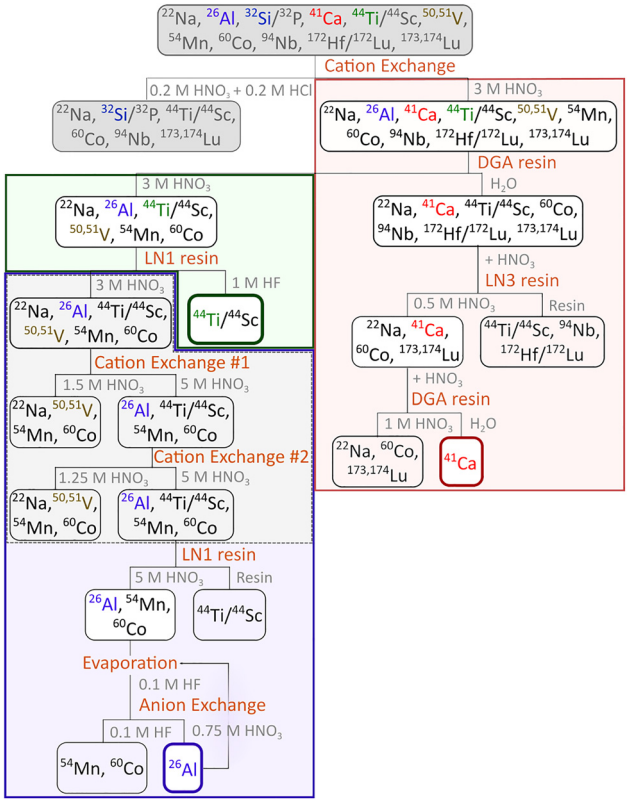

Figure 1: Full separation schematic starting from the initial vanadium target solution and ^{32}Si separation (gray) [1]. Highlighted in red are the ^{41}Ca separations: vanadium removal with DGA resin, purification #1 with LN3 resin, and purification #2 and concentration with DGA resin. In green is the ^{44}Ti separation: vanadium removal with LN1 resin. Finally, in purple are the ^{26}Al separations: Two-step vanadium removal with cation exchange resin, purification #1 with LN1 resin, concentration via evaporation, and purification #2 with anion exchange resin. The evaporation and 2nd purification are repeated. Figure 2 is a more detailed display of the two-step vanadium removal (dashed gray within the purple). The final fractions are bolded in their respective colors.

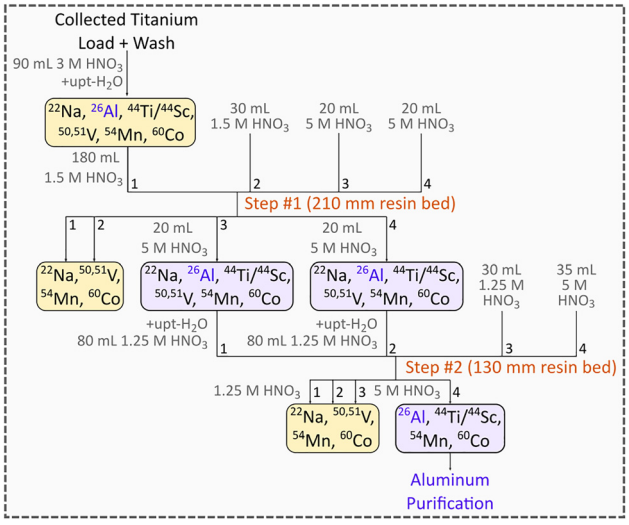

Figure 2: Separation scheme of aluminum from the vanadium matrix using two cation-exchange resin bed heights. Step #1 shows how the elute was collected in two fractions, then diluted and used as the Load for step #2. Shown is the expanded dashed gray section of Figure 1.

1.25 M HNO_3; Wash, 30 mL 1.25 M HNO_3; then Elute, 35 mL 5 M HNO_3. The Elute was collected as the separated ^{26}Al-fraction and used for further purification; the Load and Wash were discarded. For both cation exchange separations, upt-H_2O was the post-conditioning until pH = 4. This was followed by 20 mL 1.5 M or 1.25 M HNO_3 for Step #1 and #2, respectively.

Following the separation from vanadium, the ^{26}Al-fraction was subjected to two purifications and one concentration step (see Figure 1). The collected Elute, 35 mL 5 M HNO_3, was used directly as the Load for a first purification using the LN1 extraction resin (bed height: 30 mm). The resin was preconditioned with 10 mL 5 M HNO_3, proceeded by the 35 mL Load and 10 mL 5 M HNO_3 Wash, collected together for the next step. Post-conditioning consisted of 10 mL upt-H_2O, 20 mL 1 M HF, 10 mL upt-H_2O, and 10 mL 5 M HNO_3.

The second purification required a matrix change from HNO_3 to HF. This was achieved via evaporation which additionally served as a concentration step. On a PTFE evaporation dish, the collected Load and Wash from the first purification (45 mL 5 M HNO_3) was evaporated to dryness. The equivalent of three vanadium target solutions were concentrated to one solution, i.e., 135 mL 5 M HNO_3. The solid residue was then dissolved in 5 mL 1 M HF and upt-H_2O was added to reach a final concentration of 0.1 M HF that was used as Load for the second purification step.

A 30 mm bed height anion-exchange resin was preconditioned with 15 mL 0.1 M HF. This was followed by: 50 mL Load, 10 mL 0.1 M HF Wash, and then 20 mL 0.75 M HNO_3 Elute. For post-conditioning, 10 mL 1 M HF, 20 mL upt-H_2O, and 15 mL 0.1 M HF were used. For the final purification, the Elute was once more evaporated to dryness before repeating the anion-exchange separation.

3 Results and discussion

The qualitative γ-ray spectra of ^{41}Ca, ^{44}Ti, and ^{26}Al after successful separation from the irradiated vanadium targets are shown in the following section. Unless otherwise stated, the obtained fractions were measured with the varying full volumes and normalized against respective acquisition time. Stated recovery yields are calculated from the nonradioactive method development with ICP–OES. For detailed elution profiles, see the SI.

3.1 Calcium

DGA resin is well-known to retain calcium in nitric acidic environments [20, 23] and elute out in water [24]. Vanadium was removed from calcium by a factor of 19.91 (0.05) × 10^4 while calcium was recovered at 99.8% ± 2%. As previously mentioned, ^{41}Ca is a non-γ-ray emitting nuclide, thus, γ-ray spectrometry was used to trace contaminants. The targeted impurities were ^{22}Na, ^{44}Ti/^{44}Sc, ^{60}Co, ^{94}Nb, ^{172}Hf/^{172}Lu, and ^{173,174}Lu, shown in Figure 3 (Spectrum 1). The only predicted contaminants after separation through DGA resin were ^{173,174}Lu (SM Figures 2), ^{172}Hf, and ^{94}Nb [23]. Nonetheless, multiple other radionuclides were additionally seen, e.g., ^{22}Na and ^{60}Co. For titanium, some retention is possible on DGA resin at 3 M HNO_3 [23], but this was not seen in the model elution profiles (SM Figure 2). The results of the model break-through curves can be attributed to the detection limit of the ICP–OES, which is much higher as opposed to γ-spectrometric measurements.

The first purification, using the LN3 extraction resin, removed Hf(IV), Lu(III), and Ti(IV) entirely but Nb(V) only partially. Between the different available LN extract resins (LN1, LN2, and LN3), Ca(II) retains the least for any given nitric

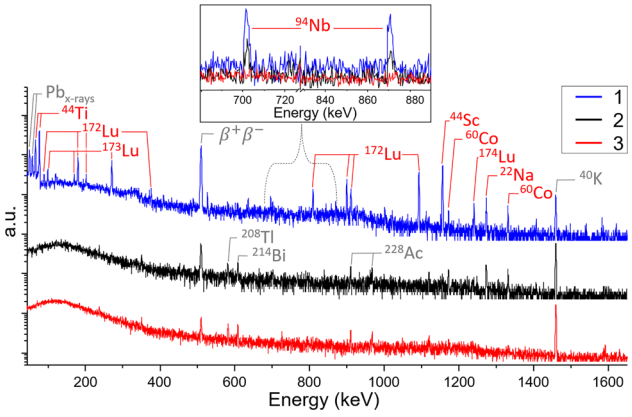

Figure 3: The γ-ray spectra of ^{41}Ca solutions after: (1) separation from vanadium on DGA resin, ^{22}Na, ^{44}Ti/^{44}Sc, ^{60}Co, ^{94}Nb, ^{172}Lu/^{172}Hf, and ^{173}Lu remain; (2) separation from ^{44}Ti/^{44}Sc, ^{172}Lu/^{172}Hf, and ^{173}Lu on LN3 resin, where ^{22}Na, ^{60}Co, and ^{94}Nb remaining; (3) separation of ^{22}Na, ^{60}Co, and ^{94}Nb on DGA resin. The sub-spectra shows the energy range of ^{94}Nb, notably its absence in the final solution.

acid concentration in LN3, whereas Hf(IV), Ti(IV), and Nb(V) retain in all concentrations of HNO_3 for all LN resins. Lu(III) has moderate retention at 0.1 M HNO_3, and Ca(II) has no retention at the same concentration [25]. Thus, it was chosen as the Load concentration. The successful removal of ^{172}Hf ($t_{1/2}$ = 1.87 (3) yr) was tracked by the daughter's γ-ray emission (^{172}Lu, $t_{1/2}$ = 6.70 (3) days) multiple weeks after separation [26]. The purification with LN3 resin successfully removed ^{44}Ti/^{44}Sc, ^{173,174}Lu, and ^{172}Hf/^{172}Lu, see Figure 3 (Spectrum 2).

For the final purification and concentration step, the reported maximum retention for calcium on DGA resin, 1 M HNO_3, was the chosen condition for the Load [23]. All remaining contaminants, ^{22}Na, ^{60}Co, and ^{94}Nb, were successfully removed, and the final spectra matched a measured background spectrum (see Figure 3, spectrum 3). For this purification, calcium was recovered at 100% ± 0.7% with an average of 5 kBq/g. Finally, the successful separation and average activity concentration of ^{41}Ca was verified by LSC (see SM Figure 4).

3.2 Titanium

The LN1 extraction resin was found to be the most reliable for separating titanium from the vanadium matrix in 3 M HNO_3 [25]. Titanium was recovered at 98.8% ± 0.2% and vanadium was removed by a decontamination factor of 6.99 (0.1) × 10^4. Although traces of ^{44}Ti were found in the ^{41}Ca-fraction and in the Load for the aluminum separation, the majority was collected in the ^{44}Ti Elute. Because of its high activity, a 5 mL aliquot of the 20 mL Elute was used for γ-ray analysis (see Figure 4). In addition to vanadium, ^{22}Na and ^{60}Co were successfully removed with LN1 resin and no other γ-ray emitting nuclides were found. The average activity concentration of ^{44}Ti being 100–200 kBq/g.

3.3 Aluminum

Due to the large concentration ratio between the vanadium and aluminum in solution and their similar retention behavior on cation-exchange resins [27], a two-step approach was chosen to remove the vanadium matrix. The applied separation scheme, with a split collected Elute, proved successful for maximum aluminum separation from vanadium while minimizing the radioactive waste (see SM Figures 6 and 7). Aluminum was recovered at 99.6% ± 0.3% and vanadium removed by a factor of 5.99 (0.01) × 10^6 following the second step. After both cation-exchange steps, ^{44}Ti/^{44}Sc, ^{54}Mn, and ^{60}Co remain as contaminants (see Figure 5).

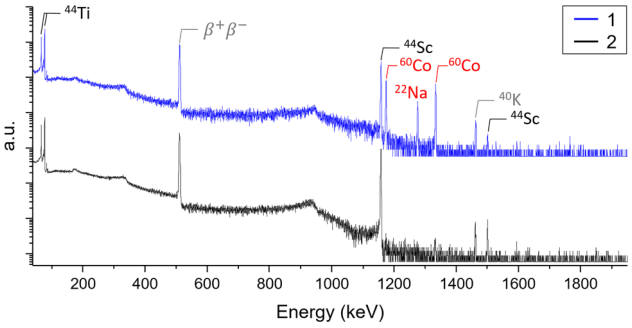

Figure 4: The γ-ray spectra of 3 M HNO_3 load (1) and 1 M HF elute (2) of the titanium separation on LN1 extraction resin. Note the daughter's emission (^{44}Sc) at 1157 and 1499 keV [4].

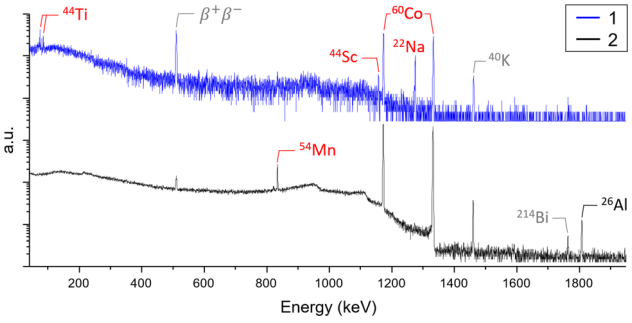

Figure 5: The γ-ray spectra of ^{26}Al before (1) and after (2) the vanadium separation with both cation exchange resin columns.

Regarding the distribution coefficients (K_d) for Ti(IV), Mn(II), and Co(II), it is expected that small quantities are still present after cation-exchange since their K_d values are between V(IV) and Al(III) [27]. As seen previously, LN1 extraction resin removed ^{44}Ti, thus it was used as the first purification step for ^{26}Al, before addressing ^{54}Mn and ^{60}Co. However, since the LN1 extraction resin does not retain Mn(II), Co(II), nor Al(III) under the chosen conditions [25], a different approach was necessary to separate these nuclides.

The separation of aluminum was achieved by converting aluminum into an anionic complex ($[AlF_4]^-$). At low HF concentrations $[AlF_4]^-$ is retained on anion-exchange resins, while Mn(II) and Co(II) are not [28, 29]. Contrary to the model experiments where aluminum was recovered at 100% ± 2% and all contaminants removed (SM Figure 9), traces of ^{54}Mn and ^{60}Co were still visible after the separation. As a result, approximately 80% of both contaminants were removed, while ^{26}Al was quantitatively recovered. Consequently, a repetition of the evaporation and subsequent separation on the anion-exchange resin removed the remaining ^{54}Mn and ^{60}Co (see Figure 6). The average activity concentration was 5–10 Bq/g.

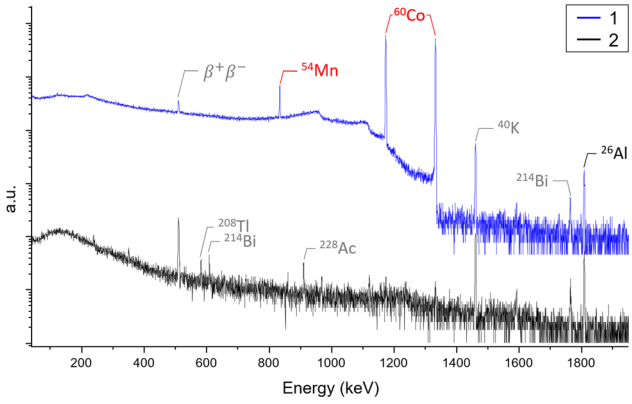

Figure 6: The γ-ray spectra of ^{26}Al after concentration via evaporation (1) and the final ^{26}Al fraction after the second anion-exchange separation (2).

4 Conclusions

Rare and exotic isotopes such as ^{41}Ca, ^{44}Ti, and ^{26}Al, are urgently needed for applications in nuclear medicine or nuclear astrophysics. Usually, their production is very challenging, but these nuclides have been identified in exceptionally high quantities as by-products due to proton-induced spallation of metallic vanadium targets. Here, the development of a selective and robust chromatographic separation method has proven to successfully isolate ^{41}Ca, ^{44}Ti, and ^{26}Al from the vanadium matrix. In the process of developing the optimal separation conditions, inactive model solutions, precisely matching the expected matrix composition, were analyzed using ICP–OES. For the radioactive solutions, the separation procedure was carried out without the addition of stable carriers. Consequently, the ^{41}Ca, ^{44}Ti, and ^{26}Al were obtained as no-carrier-added. The radiochemical purity of the final fractions was confirmed by γ-ray spectrometry and LSC. Thus, vanadium targets should be considered as candidates for long-term irradiations to provide a variety of no-carrier-added rare isotopes. In particular, a sufficiently high amount of "ready-for-use" ^{44}Ti can be provided for the development of a future radionuclide generator system as well as other exotic radioisotopes, i.e., ^{41}Ca and ^{26}Al, for instrument calibration or dedicated studies on their own.

Author contributions: All the authors have accepted responsibility for the entire content of this submitted manuscript and approved submission.

Research funding: This project is funded by the Swiss National Science Foundation (SNSF) as part of SINCHRON (No. 177229) and received additional financial support from the European Union Horizon 2020 program under Marie Skłodowska-Curie grant agreement No. 701647.

Conflict of interest statement: The authors declare no conflicts of interest regarding this article.

References

1. Veicht M., Mihalcea I., Cvjetinovic Đ., Schumann D. Radiochemical separation and purification of non-carrier-added silicon-32. *Radiochim. Acta* 2021, *109*, 735–741.
2. Woosley S. E., Heger A., Weaver T. A. The evolution and explosion of massive stars. *Rev. Mod. Phys.* 2002, *74*, 1015–1071.
3. Iyudin A. F., Schonfelder V., Bennett K., Bloemen H., Diehl R., Hermsen W., Lichti G. G., van der Meulen R. D., Ryan J., Winkler C. Emission from Ti-44 associated with a previously unknown Galactic supernova. *Nature* 1998, *396*, 142–144.
4. Chen J., Singh B., Cameron J. A. Nuclear data sheets for A=44. *Nucl. Data Sheets.* 2011, *112*, 2357–2495.
5. Besmehn A., Hoppe P., Ott U. Search for extinct aluminum-26 and titanium-44 in nanodiamonds from the Allende CV3 and Murchison CM2 meteorites. *Meteorit. Planet. Sci.* 2011, *46*, 1265–1275.
6. Travaglio C., Gallino R., Amari S., Zinner E., Woosley S., Lewis R. S. Low-density graphite grains and mixing in type II supernovae. *Astrophys. J.* 1999, *510*, 325–354.
7. Filosofov D. V., Loktionova N. S., Rosch F. A Ti-44/Sc-44 radionuclide generator for potential application of Sc-44-based PET-radiopharmaceuticals. *Radiochim. Acta* 2010, *98*, 149–156.
8. Nesaraja C. D., McCutchan E. A. Nuclear data sheets for A=41. *Nucl. Data Sheets.* 2016, *133*, 1–219.
9. Raisbeck G. M., Yiou F. Possible use of Ca-41 for radioactive dating. *Nature* 1979, *277*, 42–44.
10. Elmore D., Bhattacharyya M. H., Sacco-Gibson N., Peterson D. P. Calcium-41 as a long-term biological tracer for bone resorption. *Nucl. Instrum. Methods B.* 1990, *52*, 531–535.
11. Dong K. J., Lu L. Y., He M., Ouyang Y. G., Xue Y., Li C. L., Wu S. Y., Wang X. G., Shen H. T., Gao J. J., Wang W., Chen D. F., Xing Y. G., Yuan J., Jiang S. Study on bone resorption behavior of osteoclast under drug effect using Ca-41 tracing. *Nucl. Instrum. Methods B* 2013, *294*, 671–674.
12. Henning W., Bell W. A., Billquist P. J., Glagola B. G., Kutschera W., Liu Z., Lucas H. F., Paul M., Rehm K. E., Yntema J. L. Ca-41 concentration in terrestrial materials - prospects for dating of pleistocene samples. *Science* 1987, *236*, 725–727.
13. Basunia M. S., Hurst A. M. Nuclear Data Sheets for A=26. *Nucl. Data Sheets.* 2016, *134*, 1–148.
14. Mahoney W. A., Ling J. C., Jacobson A. S., Lingenfelter R. E. Diffuse galactic gamma-ray line emission from nucleosynthetic Fe-60, Al-26, and Na-22 – preliminary limits from heao-3. *Astrophys. J.* 1982, *262*, 742–748.
15. Lal D., Peters B. Cosmic ray produced radioactivity on the earth. In *Kosmische Strahlung II/Cosmic Rays II*; Flügge S., Ed. Encyclopedia of Physics: Berlin, Germany, Vol. XLVI/2, 1967; p. 551.
16. Balco G. Production rate calculations for cosmic-ray-muon-produced Be-10 and Al-26 benchmarked against geological calibration data. *Quat. Geochronol.* 2017, *39*, 150–173.
17. Auer M., Wagenbach D., Wild E. M., Wallner A., Priller A., Miller H., Schlosser C., Kutschera W. Cosmogenic Al-26 in the atmosphere and

the prospect of a Al-26/Be-10 chronometer to date old ice. *Earth Planet Sci. Lett.* 2009, *287*, 453–462.
18. Balco G., Shuster D. L. Al-26-Be-10-Ne-21 burial dating. *Earth Planet Sci. Lett.* 2009, *286*, 570–575.
19. Veicht M., Kajan I., David J. C., Chen S., Strub E., Mihalcea I., Schumann D. Experiment-based determination of the excitation function for the production of Ti-44 in proton-irradiated vanadium samples. *Phys. Rev. C* 2021, *104*, 014615-1-014615-10.
20. Veicht M., Mihalcea I., Gautschi P., Vockenhuber C., Maxeiner S., David J. C., Chen S. H., Schumann D. Radiochemical separation of Al-26 and Ca-41 from proton-irradiated vanadium targets for cross-section determination by means of AMS. *Radiochim. Acta* 2022, *110*, 809–816.
21. Wagner W., Seidel M., Morenzoni E., Groeschel F., Wohlmuther M., Daum M. PSI status 2008-Developments at the 590 MeV proton accelerator facility. *Nucl. Instrum. Methods A* 2009, *600*, 5–7.
22. Kiselev D., Lorenz T., Dai Y., David J. C., Schumann D., Wohlmuther M. Po-production in lead: calculation and measurement on SINQ-samples (PSI). *SATIF* 2014, *12*, 134–148.
23. Pourmand A., Dauphas N. Distribution coefficients of 60 elements on TODGA resin: application to Ca, Lu, Hf, U and Th isotope geochemistry. *Talanta* 2010, *81*, 741–753.
24. Feng L. P., Zhou L., Yang L., DePaolo D. J., Tong S. Y., Liu Y. S., Owens T. L., Gao S. Calcium isotopic compositions of sixteen USGS reference materials. *Geostand. Geoanal. Res.* 2017, *41*, 93–106.
25. McAlister D. R., Horwitz E. P. Characterization of extraction of chromatographic materials containing bis(2-ethyl-1-hexyl) phosphoric acid, 2-ethyl-1-hexyl (2-ethyl-1-hexyl) phosphonic acid, and bis(2, 4, 4-trimethyl-1-pentyl) phosphinic acid. *Solvent Extr. Ion Exch.* 2007, *25*, 757–769.
26. Singh B. Nuclear data sheets for A = 172. *Nucl. Data Sheets* 1995, *75*, 199–376.
27. Strelow F. W. E., Rethemey R., Bothma C. J. C. Ion exchange selectivicity scales for cations in nitric acid and sulfuric acid media with A sulfonated polystyrene resin. *Anal. Chem.* 1965, *37*, 106.
28. Faris J. P. Adsorption of the elements from hydrofluoric acid by anion exchange. *Anal. Chem.* 1960, *32*, 520–522.
29. Faris J. P., Buchanan R. F. Anion exchange characteristics of elements in nitric acid medium. *Anal. Chem.* 1964, *36*, 1157.

Supplementary Material: This article contains supplementary material (https://doi.org/10.1515/ract-2022-0072).